LITERATURE REVIEW

Earthquake Effect

Seismic design of high bridges shall be clarified in AASHTO code based on acceleration coefficients (A) for the seismic zone as shown in the seismic risk map and is indicated in Table 1. The earthquake loads shall be applied as the horizontal force exerted on bridge structure. Earthquake loads are given by the product of the elastic response coefficient and equivalent weight of the super structure. The coefficient depends on parameter such as period of vibration, acceleration coefficient and site coefficient. The equivalent weight is a function of the actual weight and bridge configuration including both the single- mode and multi-mode methods of analysis. The actual ductility demand on the column or pier is a complex function of various variables.

Table 1 Seismic performance category (SPC)

Acceleration Coefficient (A)	Seismic Zone	Importance Classification (IC)	
		I	II
$A \leq 0.09$	1	A	A
$0.09 < A \leq 0.19$	2	B	B
$0.19 < A \leq 0.29$	3	C	C
$0.29 < A$	4	D	C

Source: AASHTO (1996)

For bridges classified as Seismic Performance Category B, C or D, the seismic analysis is required. The earthquake effects shall be determined from applying horizontal ground motion in two orthogonal directions along global axes. The longitudinal axis is typically represented by a chord connecting the two abutments. The two load cases are as follows:

Load Case 1: To combine the response resulting from the application of 100% of the transverse loading and 30% of the concurrent longitudinal loading.

Load Case 2: To combine the response resulting from the application of 100% of the longitudinal loading and 30% of the concurrent transverse loading.

For design forces for seismic performance category (SPC) A, the connection of the substructure shall be designed resisting horizontal seismic force equally 20% of the dead load reaction force in the restrained direction.

For design forces for SPC- B, SPC-C and SPC-D, the design forces for structural members and connections shall be designed for the modified seismic forces resulting from the two load cases combined independently with forces from other loads specified in the following group loading combination for the components. Each component shall be calculated as in Equation 1 of AASHTO code.

$$\text{Group load} = 1(D+B+SF+E+EQM) \quad (1)$$

where

D = dead load

B = buoyancy

SF = stream-flow pressure

E = earth pressure

EQM = elastic seismic force for either Load Case 1 or Load Case 2

For service load design, a 33% increase of allowable stress is permitted for reinforced concrete.

For SPC-C and SPC-D, the force resulting from plastic hinging at the top and bottom of

the column shall be calculated after the preliminary design of the columns is complete. For the reinforced concrete column use a strength reduction factor (ϕ) of 1.25 times the nominal yield strength.

According to American Association of State Highway and Transportation Officials (AASHTO 1996), bridge design for Seismic Zone 1 need not be analyzed for seismic loads because of the low level of seismic risk. However the minimum requirement for bridge seat widths at expansion bearing shall be required for longitudinal movement. For Seismic Zone 2, the seismic force will cause yielding of the bridge column which shall be considered. Thus it is necessary for the columns to have some ductility capacity to prevent buckling of longitudinal steel and provide confinement for core of the column. The maximum spacing for the transverse reinforcement is 152 mm. Bridges in Seismic Zone 3 and 4 more need more ductility demands. The area of longitudinal reinforcement shall be limited between 0.01 and 0.06. The design maximum axial force is $0.2f_c^{'}A_g$. The cores of columns shall be provided with transverse reinforcement in the plastic hinge region. The minimum total cross-section area of rectangular hoops reinforcement shall be less than either Equation (2) and (3). The maximum spacing for the transverse reinforcement is 100 mm.

$$\frac{A_{sh}}{sh_c} = 0.3\frac{f_c^{'}}{f_{yh}}\left(\frac{A_g}{A_{ch}} - 1\right) \tag{2}$$

$$\frac{A_{sh}}{sh_c} = 0.12\frac{f_c^{'}}{f_{yh}} \tag{3}$$

As a result of the 1971 San Fernando, California earthquake during which many highway bridges were severely damaged, some of which even collapsed, the California Department of Transportation (Caltrans) issued new seismic design criteria for bridges in 1973, which formed the basis of the AASHTO Interim Specifications for Highway Bridges (1975). The equivalent static lateral force loading specified applied to the horizontal direction. The same seismic design criteria in the 1975 Interim Specifications were repeated in the Twelfth (1977), Thirteenth (1983), and Fourteenth (1989) Editions of AASHTO's Standard Specifications. However in these

editions, the designer was given, the choice of working-stress design (WSD) or load-factor design (LFD). When using the WSD the increase 33.33% of allowable stress is permitted for service load design. However when using the LFD, the load factor was assigned the value 1.3 produced in the Group load combination.

During the period 1988 to 1993, the AASHTO LRFD Bridge Design Specifications was developed using statistically based probability methods. The load and resistance factor design (LRFD) philosophy makes use of load and resistance factors developed through statistical analyses. The AASHTO LRFD Bridge Design Specifications, First (1994) and Second (1999) Editions, require that each bridge component and connection satisfy all limit states.

Development of Structural Behavior under Seismic Loading

The strength and ductility of concrete under tri-axial compression is shown in Fig. 4 (Richart et al., 1928). This figure presents stress-strain curves for concrete cylinders subjected to a constant lateral confining fluid pressure while the longitudinal stress was increased to failure. The relationship of axial stress and confining pressure in given by

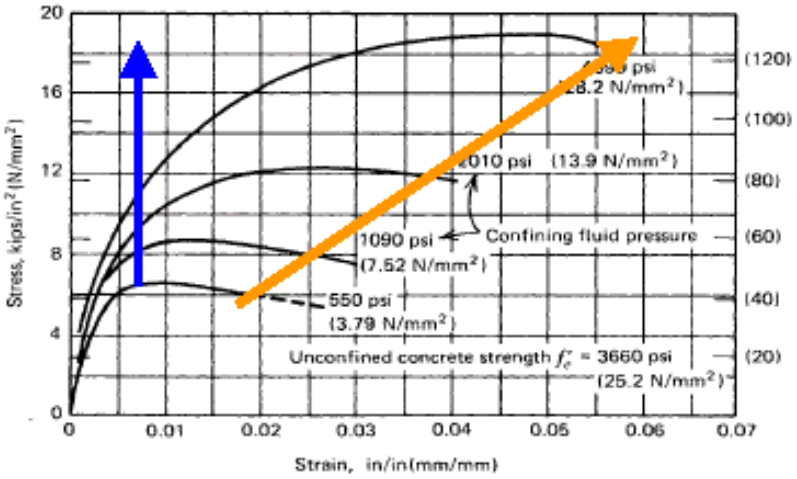

Figure 4 Axial stress-strain curves from tri-axial compression

Source: Richart et al. (1928)

$$f_{cc} = f_c^{'} + 4.1 f_l \tag{4}$$

where

f_{cc} = the longitudinal stress at failure

$f_c^{'}$ = the uniaxial compressive strength

f_l = the confining pressure

For spirals hoop shape placed in hoop tension, as the concrete expands under uniaxial compression loading it provides a continuous confining line load around the circumference of the enclosed concrete. The maximum effective lateral pressure, f_l, on the concrete occurs when the spirals or hoops reach their yield strength, f_{yh}. From the Fig. 5, equilibrium required is shown in Equation (5) (Paulay and Priestley, 1992).

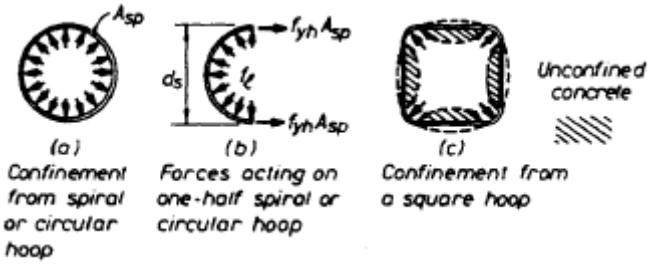

Figure 5 Mechanism of confining line load under compression loading

Source: Paulay and Priestley (1992)

$$f_l = \frac{2 f_{yh} A_{sp}}{d_s s_h} \tag{5}$$

where

d_s is the diameter of the hoop or spiral, which has a cross-sectional area of A_{sp}, and s_h is the longitudinal spacing of the hoops or the pitch on the spirals. The square hoops, they are not as effective as circular hoops but are only fully effective near the corners of the hoops. As such for

the effectiveness of the confining reinforcement, the efficiency function *R* is 1.0 for spiral and 0.5 for hoop reinforcement (Paulay and Priestley, 1992).

As shown in Fig. 6, the ratio of the maximum concrete strain in confined and unconfined concrete can range between 4 and 15, which indicates the substantial benefit of confining concrete in zones of the concrete structure that will dissipate energy.

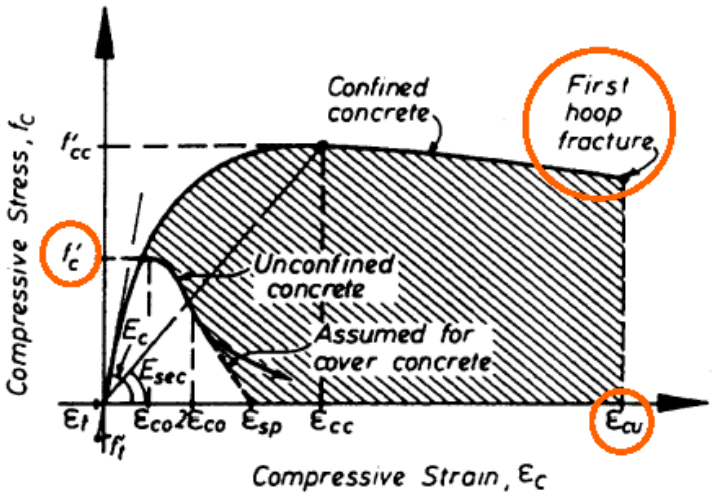

Figure 6 Stress vs. strain relationship of confined and unconfined concrete

Source: Mander et al. (1988a, b)

Mander et al. (1988a, b) proposed the peak stress and confined strain at peak stress of the confined concrete following Equation (6) and (7).

$$f_{cc} = f_c^{'}\left(2.254\sqrt{1+\frac{7.94 f_l^{'}}{f_c^{'}}}-\frac{2 f_l^{'}}{f_c^{'}}-1.254\right) \tag{6}$$

$$\varepsilon_{cc} = 0.002\left\{1+5\left(\frac{f_{cc}^{'}}{f_c^{'}}-1\right)\right\} \tag{7}$$

$$f_l^{'} = K_e\left(\frac{2 f_{yh} A_{sp}}{d_s s_h}\right) \tag{8}$$

where

K_e = the confinement effectiveness coefficient related to the area of the effectively confined core

Typical values for K_e are 0.95 for circular section, 0.75 for rectangular section and 0.6 for rectangular wall section.

Kawashima et al., 2001 presented a cyclic loading test of three specimens of full sized bridge piers. The first specimen (Type A) was designed according to the 1980 Design Specification of Highway Bridges based on the working stress design approach. The vertical reinforcement ratio and volumetric tie reinforcement ratio were 0.74% and 0.56% respectively. The second (Type B) specimen was design according to the 1996 Design Specification of Highway Bridges. Although the vertical reinforcement was the same as the Type-A, the volumetric tie reinforcement ratio was increased to 0.91% by increasing the number of ties. The third specimen (Type C) was an interlocking spiral column. The vertical reinforcement ratio was increasing to 0.83% and volumetric tie reinforcement ratio was almost the same as the Type-B Specimen. Cross section of test specimens are shown in Fig. 7 and lateral force vs. lateral displacement hysteresis is shown in Fig. 8. The specimens were subjected to a cyclic lateral loading under a constant vertical load.

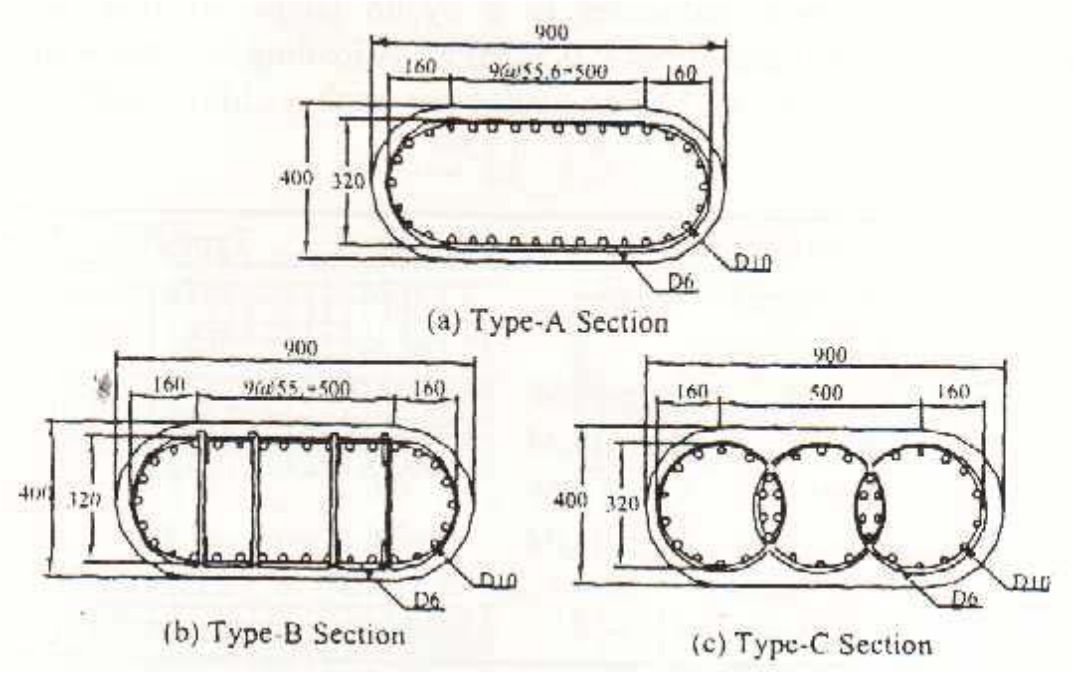

Figure 7 Sections of Specimens

Source: Kawashima et al. (2001)

The following conclusions were presented as follows:

1. The Type-A specimen failed in shear, the shear capacity obtained in the test can be directly compared with the computed result. On the other hand, since the Type-B and C specimens failed in flexure, the shear capacity was larger than the flexural capacity obtained in the test.
2. The Type B and Type C Specimens provided similar plastic deformation and energy dissipation capacity.
3. The shear capacities based on Japan Road Association 1996 (JRA) , Japan Society of Civil Engineering 1997 (JSCE), and the Shear Strength of Reinforced Concrete Members (ASCE-ACI Task Committee 426 , 1973) are close to each other, and provide reasonable estimation to the test result. The shear capacity proposed by Priestley et al. (1994) provides the most reasonable evaluation.

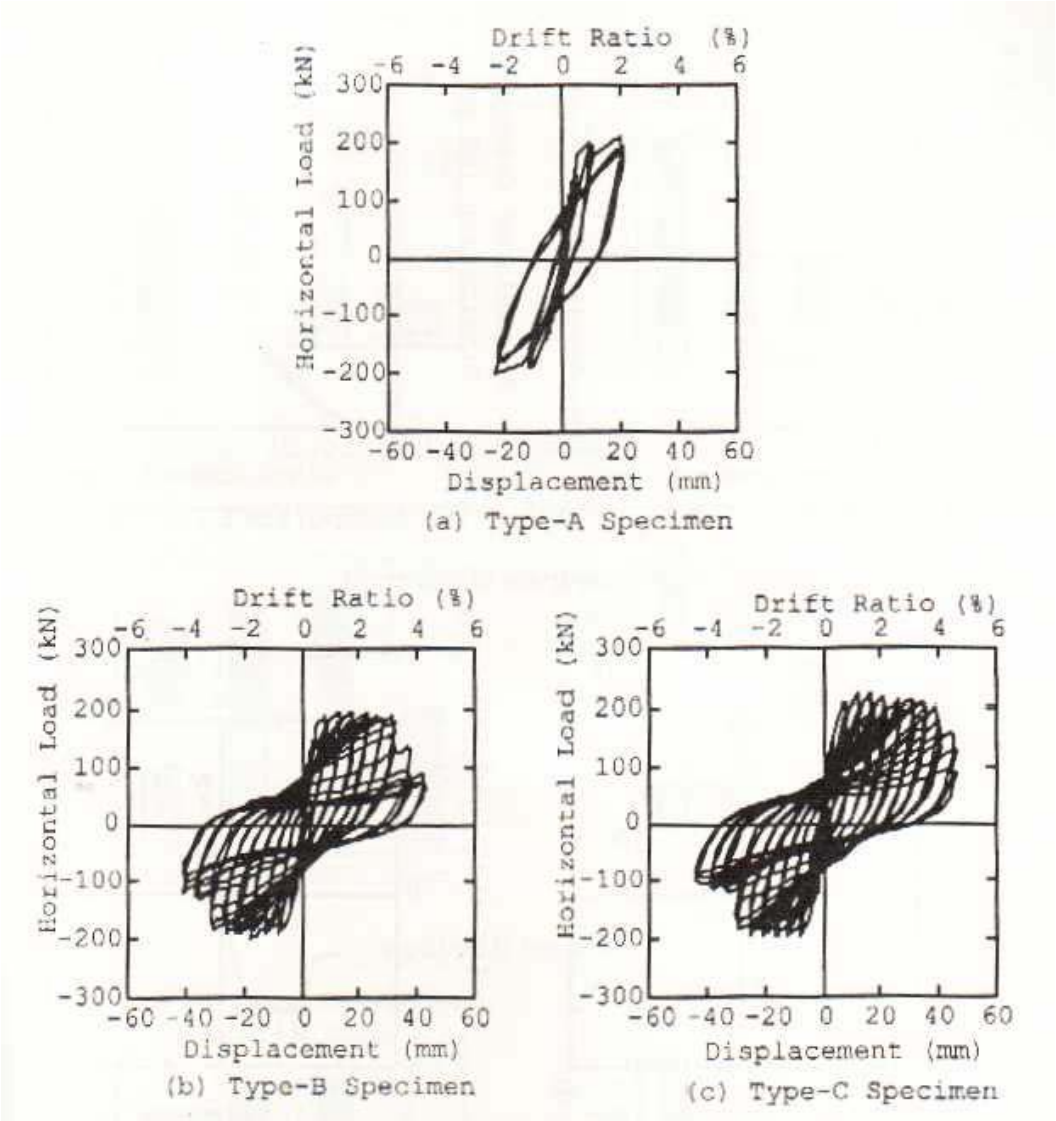

Figure 8 Lateral force vs. lateral displacement hysteresis

Source: Kawashima et al. (2001)

Jae et al. (2001) investigated the seismic behavior and capacity of reinforced concrete piers that were not detailed for seismic load. Two types of prototype piers, solid circular section with 1 m diameter and 5.0 m height and hollow rectangular section with 1.04 m × 0.60 m cross section and 5.0 m height are considered. Two kinds of reinforcement details, lap spliced and continuous are considered for the vertical longitudinal reinforcing bars. In the case of lap spliced model all the longitudinal bars were lap spliced at the same height in the bottom plastic hinge zone. Four specimens were constructed, two of circular section and two of hollow rectangular

section. They were subjected to quasi-static cyclic lateral loading while the vertical load held constant. In the case of solid circular section, the failure of the lap spliced model was not ductile but the failure of continuous bar model was limited ductile. In the case of hollow rectangular section, the failure of the lap-spliced model was limited ductile but the failure of continuous bar model was ductile. Comparison of envelope curves is shown in Fig. 9.

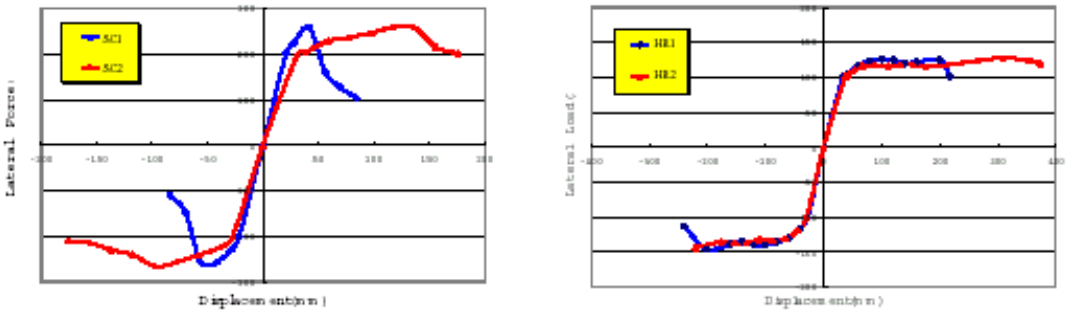

(a) Solid circular column (b) Hollow rectangular column

Figure 9 Comparison of envelope curves

Source: Jae et al. (2001)

Sakai and Kawashima (2000) presented uniaxial compressive loading tests on concrete cylinder confined by tie reinforcements in order to develop an unloading and reloading stress-strain model. The specimens were 600 mm height and 200 mm in diameter with various volumetric ratios of tie strength and cylinder strength of concrete. The tie reinforcement ratio, ρ_s and the cylinder strength of concrete were varied from 0.67% to 2.67% and from 23 MPa to 36.7 MPa, respectively. The detail of test specimen series is shown in Table 2.

Table 2 **Test series of Sakai and Kawashima (2000)**

Test series	Cylinder strength of concrete, f_{co} (MPa)	Tie reinforcement	
		Spacing, S (mm)	Volumetric ratio (%)
A	23.0	100	0.67
B		50	1.33
C		25	2.67
D	36.7	60	1.14
E	29.8		

Source: Sakai and Kawashima (2000)

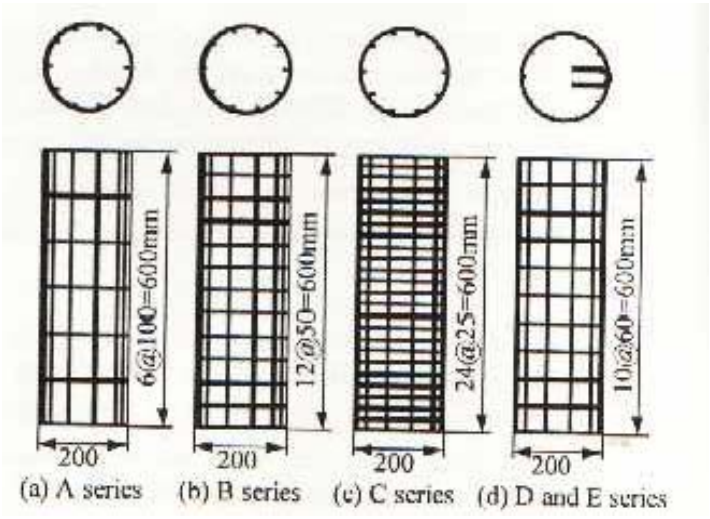

Figure 10 Tie reinforcement series

Source: Sakai and Kawashima (2000)

It was concluded that:

1. The effect of unloading and reloading on the stress-stain envelope curve is less significant.

2. The plastic strain and the stress deterioration ratio of the specimens unloaded at the same strain are less dependent on the tie reinforcement ratio or cylinder strength of concrete and provide reasonable evaluation of $\varepsilon_{pl.1}$ for an unloading part and β_1 for a reloading part.

Effect of repeating reloading and unloading hytereses was included in the stress vs. strain model of confined concrete developed by Sakai and Kawashima (2000). In this model, the reloading and unloading hytereses were idealized by a set of full unloading and full reloading. The stress vs. strain relation of concrete subjected to *n* time full unloading and full reloading are shown as

$$f_c = f_{ul.n}\left(\frac{\varepsilon_c - \varepsilon_{pl.n}}{\varepsilon_{ul} - \varepsilon_{pl.n}}\right)^2 \tag{9}$$

$$f_c = \begin{pmatrix} 2.5 f_{ul.n}\left(\dfrac{\varepsilon_c - \varepsilon_{pl.n}}{\varepsilon_{ul} - \varepsilon_{pl.n}}\right)^2 & \cdots\cdots 0 \le \bar{\varepsilon}_c < 0.2 \\ E_{rl}\left(\varepsilon_c - \varepsilon_{ul}\right) + f_{ul.n+1} & \cdots\cdots 0.2 \le \bar{\varepsilon}_c \le 1 \end{pmatrix} \tag{10}$$

where , $\bar{f}_c$ and $\bar{\varepsilon}_c$ are normalized stress and strain defined by

$$\bar{f}_c = \frac{f_c}{f_{ul.n}} \qquad \text{and} \qquad \bar{\varepsilon}_c = \frac{\varepsilon_c - \varepsilon_{pl.n}}{\varepsilon_{ul} - \varepsilon_{pl.n}} \tag{11}$$

and E_{rl} is the averaged stiffness in the reloading path between $0.2 \le \bar{\varepsilon}_c \le 1$

$$E_{rl} = \frac{f_{ul.n+1} - 0.1 f_{ul.n}}{0.8(\varepsilon_{ul} - \varepsilon_{pl.n})} \tag{12}$$

The deterioration rate of $f_{ul.n}$ and the increasing rate of $\varepsilon_{pl.n}$ are represented by

$$\beta_n = \frac{f_{ul.n+1}}{f_{ul.n}} \text{ and } \gamma_n = \frac{\varepsilon_{ul} - \varepsilon_{pl.n}}{\varepsilon_{ul} - \varepsilon_{pl.n-1}}$$

where β_n and γ_n are given as

For n = 1 and 2

$$\beta_n = \begin{pmatrix} 1 & \cdots\cdots 0 \le \varepsilon_{ul} \le 0.001 \\ 1-(10n+22)(\varepsilon_{ul}-0.001) & \cdots\cdots 0.001 < \varepsilon_{ul} < 0.003 \\ 0.92+0.025(n-1) & \cdots\cdots 0.0035 \le \varepsilon_{ul} \le 0.03 \end{pmatrix}$$

For n $\geq$ 3

$$\beta_n = \begin{pmatrix} 1 & \cdots\cdots 0 \le \varepsilon_{ul} \le 0.001 \\ 1-(2n+8)(\varepsilon_{ul}-0.001) & \cdots\cdots 0.001 < \varepsilon_{ul} < 0.0035 \\ 0.965+0.005(n-3) & \cdots\cdots 0.0035 \le \varepsilon_{ul} \le 0.03 \end{pmatrix}$$

$$\gamma_n = \begin{pmatrix} 0.945 & \cdots\cdots n = 2 \\ 0.965+0.005(n-3) & \cdots\cdots n \ge 3 \end{pmatrix}$$

where $\beta_n \leq 1$

ε_{pl} = Plastic Strain where stress becomes 0

ε_{ul} = Unloading Strain varied in the range 0 to 0.03

$= k\varepsilon_{cc}/4$ ……(k = 1, 2, …m)

ε_{cc} = strain at peak stress

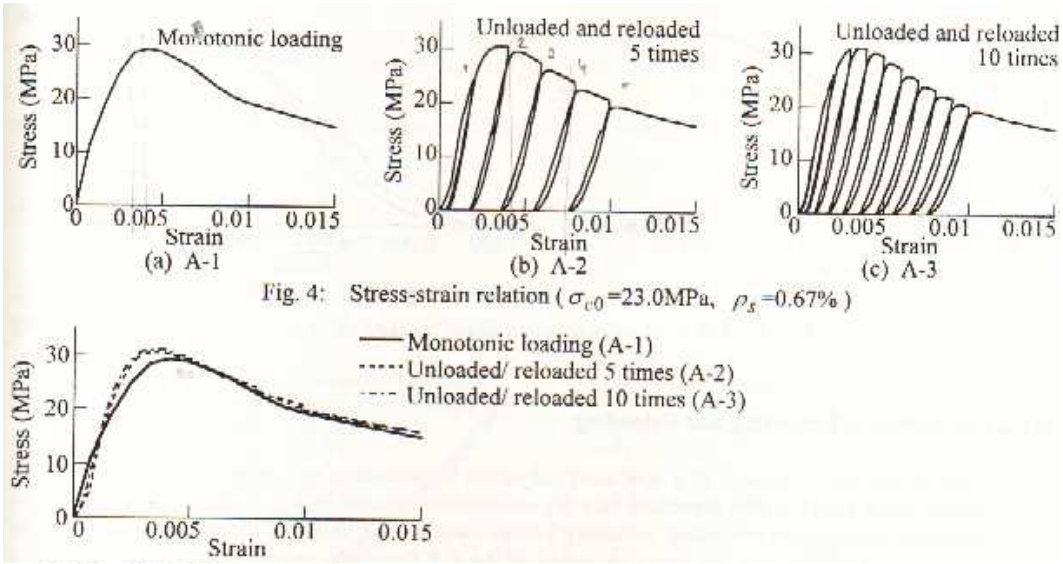

Figure 11 Effect of number of loading on envelope curve

Source: Sakai and Kawashima (2000)

Hoshikuma et al. (1997) proposed the stress vs. strain model of confine concrete shown in Fig. 12 and determined as

$$f_c = \begin{cases} E_c\varepsilon_c\left\{1-\frac{1}{n}\left(\frac{\varepsilon_c}{\varepsilon_{cc}}\right)^{n-1}\right\} & \cdots\cdots 0 \le \varepsilon_c \le \varepsilon_{cc} \\ f_{cc} - E_{des}\left(\varepsilon_c - \varepsilon_{cc}\right) & \cdots\cdots \varepsilon_{cc} < \varepsilon_c \le \varepsilon_{cu} \end{cases} \qquad (13)$$

$$n = \frac{E_c\varepsilon_{cc}}{E_c\varepsilon_{cc} - f_{cc}}$$

$$f_{cc} = f_{co} + 0.76 f_{yh}$$

$$\varepsilon_{cc} = 0.002 + 0.0132\frac{\rho_s f_{yh}}{f_{co}}$$

$$E_{des} = 11.2\frac{f_{ck}^2}{\rho_s f_{sy}}$$

$$\varepsilon_{cu} = \varepsilon_{cc} + \frac{0.8 f_{cc}}{E_{des}}$$

$$\varepsilon_{cc} = 0.00218 + 0.0332\frac{\rho_s f_{yh}}{f_{co}} \qquad \text{for circular section}$$

$$\varepsilon_{cc} = 0.00245 + 0.0122\frac{\rho_s f_{yh}}{f_{co}} \qquad \text{for square section}$$

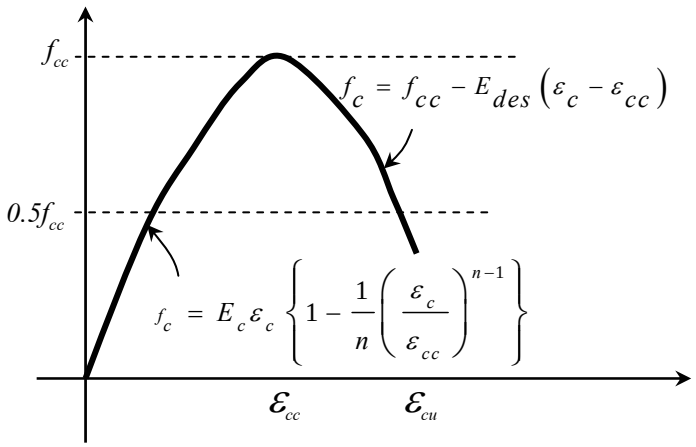

Figure 12 Stress – strain curve for confined concrete
Source: Hoshikuma et al. (1997)

For the covering concrete, the stress vs. strain model of the unconfined concrete was idealized as

$$f_c = \begin{cases} E_c\varepsilon_c\left\{1 - \frac{1}{n}\left(\frac{\varepsilon_c}{0.002}\right)^{n-1}\right\} & \cdots\cdots 0 \le \varepsilon_c \le \varepsilon_{cc} \\ \frac{f_{cc}}{0.005}\left(0.007 - \varepsilon_c\right) & \cdots\cdots \varepsilon_{cc} < \varepsilon_c \le \varepsilon_{cu} \\ 0 & \cdots\cdots \varepsilon_{cu} < \varepsilon_c \end{cases} \qquad (14)$$

Kent and Park (1971), Sheikh and Uzumeri (1980, 1982), Saatcioglu and Razvi (1992) and Fujii et al. (1988) considered the sustained stress after the falling branch to be 20 or 30% of the peak stress.

Menegoto and Pinto (1973) proposed a model for characterizing vertical reinforcing steel in which the response is defined by the following non-linear Equation 15 and Fig. 13.

$$\tilde{\sigma} = R_s\tilde{\varepsilon} + \frac{\left(1 - R_s\right)\tilde{\varepsilon}}{\left(1 + \tilde{\varepsilon}^R\right)^{1/R}} \qquad (15)$$

$$\tilde{\sigma} = \frac{\sigma_s - \sigma_r}{\sigma_o - \sigma_r}$$

$$\tilde{\varepsilon} = \frac{\varepsilon_s - \varepsilon_r}{\varepsilon_o - \varepsilon_r}$$

Where the effective strain and stress $\left(\tilde{\sigma}, \tilde{\varepsilon}\right)$ are a function of the unloading and reloading interval, ε_r, σ_r are the strain and stress at reversal point, ε_o, σ_o are the strain and stress at intersection of the asymptotes, R_s is the ratio of the initial to final tangent stiffness and R is a parameter that defines the shape of unloading curve.

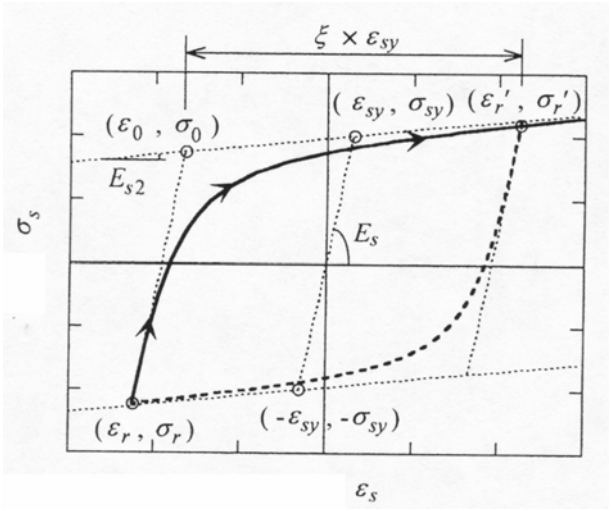

Figure 13 Stress vs. strain curve for vertical steel reinforcement

Source: Menegoto and Pinto (1973)

Lateral Steel Requirements for Rectangular Confined Columns

There are different methods for the design of confinement reinforcement. A summary of the methods for the plastic hinge region of rectangular columns is presented.

Based on American Concrete Institute (ACI 318-95) 1995, the minimum total cross-section area of rectangular hoops and crossties is the larger of

$$\frac{A_{sh}}{sh_c} = 0.3\frac{f_c^{'}}{f_{yh}}\left(\frac{A_g}{A_{ch}} - 1\right) \tag{16}$$

$$\frac{A_{sh}}{sh_c} = 0.09\frac{f_c^{'}}{f_{yh}} \tag{17}$$

where

$5 < s < 20$ cm or 1/4 of the minimum member dimension

California Association of State Highway (Caltrans 1983) provisions specify as the large one of the two expressions for the minimum area of transverse reinforcement which is

$$\frac{A_{sh}}{sh_c} = 0.3\frac{f_c^{'}}{f_{yh}}\left(\frac{A_g}{A_{ch}} - 1\right) \tag{18}$$

$$\frac{A_{sh}}{sh_c} = 0.12\frac{f_c^{'}}{f_{yh}}\left(0.5 + 1.25\frac{P}{f_c^{'}A_g}\right) \tag{19}$$

where

50 mm < s < 200 mm or 1/5 of the minimum member dimension whichever is smaller

The research on bridge columns conducted by Zahn et al., 1986 and Watson et al., 1994 proposed the designed equation and chart for relating the amount of confinement steel in the columns to the applied axial load and the required curvature ductility (μ_ϕ); the amount being simplified by Paulay and Priestley (1992) is given in following Equation (20).

$$\frac{A_{sh}}{sh_c} = k\frac{f_c^{'}A_g}{f_y A_c}\left(\frac{P}{f_c^{'}A_g} - 0.08\right) \tag{20}$$

where

s < 1/3 of the minimum member dimension, six times the longitudinal bar diameter, and 180 mm whichever is smaller

k = 0.25 when μ_ϕ = 10 and k = 0.35 when μ_ϕ = 20

The flexibility provided by including the ductility demand makes the expression useful not only for bridge columns that are in areas of high seismicity, but also for those in areas of moderate seism city where the ductility demand may be lower.

Standard Association of New Zealand (1982) specified the tie reinforcement, being the larger of steel areas from the two expressions; being functions of the axial load.

$$\frac{A_{sh}}{sh_c} = 0.3\left(\frac{A_s}{A_{ch}} - 1\right)\frac{f_c^{'}}{f_{yh}}\left(0.5 + 1.25\frac{P}{\phi f_c^{'} A_g}\right) \tag{21}$$

$$\frac{A_{sh}}{sh_c} = 0.12\frac{f_c^{'}}{f_{yh}}\left(0.5 + 1.25\frac{P}{f_c^{'} A_g}\right) \tag{22}$$

where

ϕ = strength reduction factor is equal to 0.9

s < 20 cm and 1/5 of the minimum member dimension and six times the longitudinal bar diameter, whichever is smaller.

The Bridge Design Specifications issued by the Applied Technology Council, 1996 recommends the following Equation (23) to find the minimum cross-sectional area of lateral steel in rectangular columns.

$$\frac{A_{sh}}{sh_c} = 0.12\frac{f_{ce}^{'}}{f_{ye}}\left(0.5 + 1.25\frac{P}{f_{ce}^{'} A_g}\right) + 0.13\left(\rho_l - 0.01\right) \tag{23}$$

where

ρ_l = vertical reinforcement ratio

$f_{ce}^{'}$ = expected concrete strength

f_{ye} = expected yield strength of transverse reinforcement

s < 305 mm and the least column dimension whichever is smaller

When longitudinal bars greater than ϕ32 mm are bundled, the maximum tie spacing is reduced to one-half of the specified limits

Wehbe et al., 1999 studied and developed detail guidelines for reinforced concrete bridge columns and wall for areas of low seismicity to moderate seismicity. Four specimens from half-scaled rectangular bridge columns were constructed and tested. The specimens were tested under constant axial load while subjected to quasi-static cyclic lateral loading in the column strong direction. The axial load indexes were 10% and 25 %.

The amount of confinement reinforcement was proposed in Equation (24) being function of the axial load and the target ductility. For the proportioning of moderate column confinement, it was suggested that when the target-displacement ductility ratio is 2, the lateral steel amount is nearly identical to that required by the ACI with no seismic provision. At a moderate target-displacement ductility ratio of 4, the lateral confining reinforcement is considerably less than the amount required by other seismic provisions.

$$\frac{A_{sh}}{sh_c} = 0.1\mu_\Delta \sqrt{\frac{f_{c.n}}{f_{ce}^{'}}} \left[0.12 \frac{f_{ce}^{'}}{f_{ye}} \left(0.5 + 1.25 \frac{P}{f_{ce}^{'} A_g} \right) + 0.13 \left(\rho_l \frac{f_{ye}}{f_{s,n}} - 0.01 \right) \right] \qquad (24)$$

Nominal Flexural Strength

Nominal Flexural Strength

When specimens are subjected combined axial force and a bending moment, the nominal moment capacity is depends on an axial force shown in Fig. 14 and is calculated based on equilibrium and compatibility strain relationship. The extreme compression fiber strain of concrete was assumed as ε_{cu} and concrete compressive strength was $0.85f^{'}_{c}$ shown in Fig. 14.

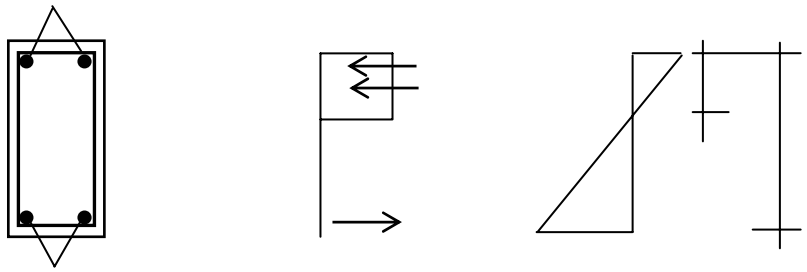

a) cross section b) stress diagram c) strain diagram

Figure 14 Stress and strain diagram for nominal moment strength

The axial load influences the curvature and moment. Blume et al. (1961) plotted the interaction diagram of axial load (P) against moment (M) and axial load (P) against curvature (φh) shown in Fig. 15 for unconfined column section having axial reinforcement on two opposite faces. Curve 1 in Fig. 15a indicates the combination of P and M that cause the column to reach the ultimate state by limiting of concrete strain at 0.004. Curve 1 in Fig. 15b shows the curvature of section corresponding to the combination of P and M when this ultimate condition is reached. Curve 2 give the combination of P, M and φh when the tension steel reaches to the yield strength. Curves 2 do not appear above the balance point on compression failure because the tension steel does not reach the yield strength. For $P - M$ diagram in Fig. 15a, below the balance point on tension failure curve 1 and curve 2 lie close together. It indicates that the load capacity changes slightly. For P - φh diagram in Fig. 15b, the curve 1 and curve 2 occurs when yielding started.

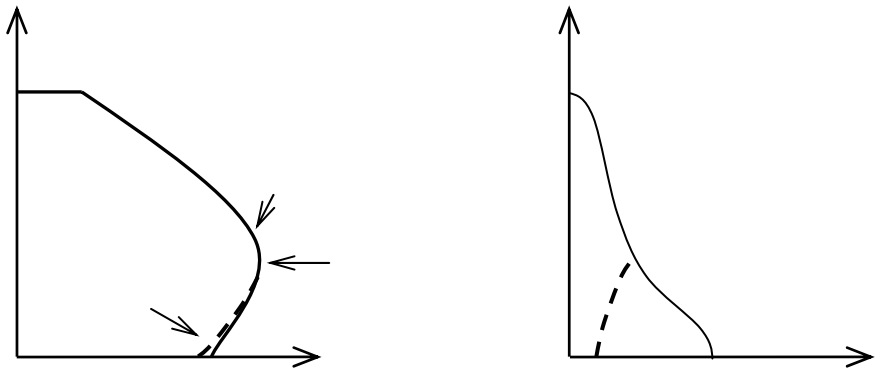

a) Axial load and moment b) Axial load and curvature

Figure 15 Strength and ductility of column

Source: Blume et al. (1961)

In a typical column which fails in flexure subjected to lateral cyclic load, the damage progresses from flexural cracks, flexural failure of concrete outward buckling of longitudinal steels, outward deformation of confinements, spall off of covering concrete and rupture of longitudinal and confinement steel.

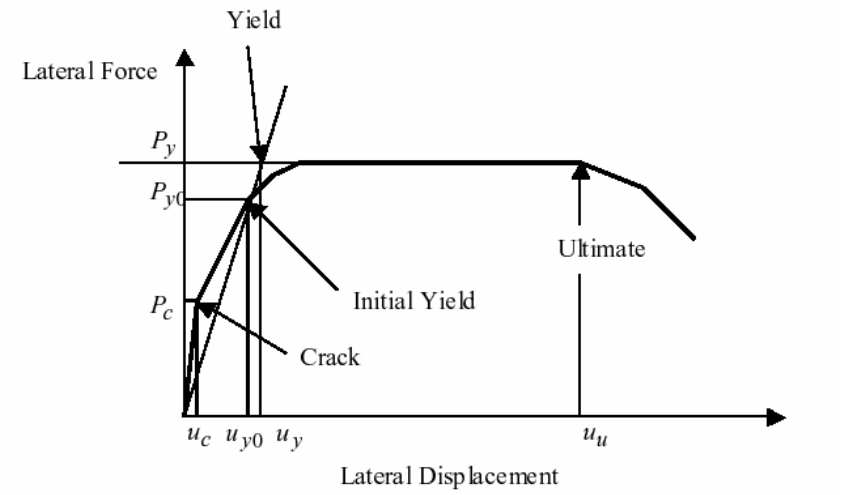

Figure 16 First yield, yield, and ultimate of a column which fails in flexure

Source: Kawashima (2003)

Fig. 16 idealizes an envelop of the lateral force vs. lateral displacement hysteresis response of columns subjected to cyclic load. The column has at first the uncracked stiffness, k_{uc} defined as Equation (25).

$$k_{uc} = \frac{P_c}{u_c} \tag{25}$$

where P_c and u_c are the lateral force and lateral displacement when flexural first cracks occur. At initial yield, (P_{y0} and u_{y0}) the column starts yield of when longitudinal steel in compression at the extreme fiber start to yield. The cracks stiffness of column is defined as Equation (26).

$$k_{cr} = \frac{P_{y0}}{u_{y0}} \tag{26}$$

As the lateral displacement increases, other rebars start to yield, and the lateral force is eventually saturated at P_y (flexural strength) when all rebars in the flexural compression zone yield. There are various ways of defining yield of a column. However, it is common to define it as an intersection between a line connecting the original rest point and the initial yield and a line of the flexural strength. Significant deterioration of lateral force occurs when one of the following failures occurs; spalling off of covering concrete, local buckling of longitudinal rebars, extensive outward deformation of ties and rupture of longitudinal rebars.

Equivalent Stiffness and Energy Dissipation

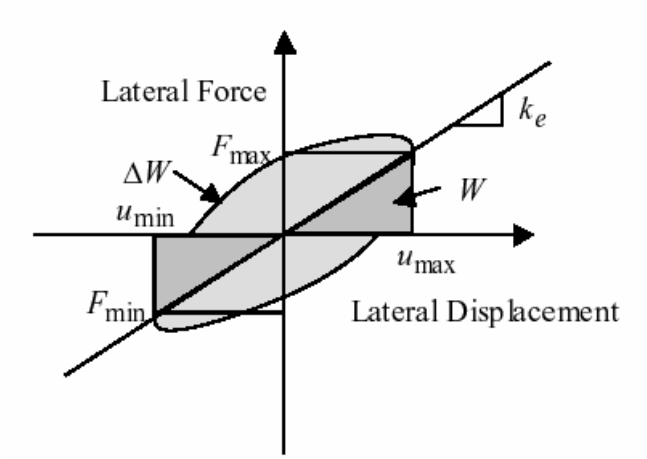

Figure 17 Equivalent stiffness and energy dissipation

Source: Kawashima (2003)

As shown in Fig. 17 an equivalent stiffness (k_e) of a column is defined for each loading step as Equation (27)

$$k_e = \frac{P_{\max} - P_{\min}}{u_{\max} - u_{\min}} \tag{27}$$

where u_{max} and u_{min} are the maximum and minimum displacements on a hysteresis and F_{max} and F_{min} are the restoring forces at u_{max} and u_{min}.

The dissipation energy during an ith load reversal is calculated by Equation (28).

$$\begin{aligned} \Delta W_i &= \int_{-u_{\max}}^{u_{\max}} F_l(u)du + \int_{u_{\max}}^{-u_{\min}} F_{ul}(u)du \\ &= \int_{-u_{\max}}^{u_{\max}} (F_l(u) - F_{ul}(u))du \end{aligned} \tag{28}$$

where $F_{l(u)}$ and $F_{ul(u)}$ represent the force at displacement (u) during loading and unloading processes. As shown in Fig. 17, ΔW_i by Equation (28) is the area of surrounded by a hysteresis. The accumulated energy dissipated in a column is then obtained as Equation (29).

$$\Delta W = \sum_i \Delta W_i \tag{29}$$

Fiber Element Method

A fiber element is designed to model the 3 dimension in the reinforced concrete member. Its cross-section can be divided into elements of steel and concrete in the axial direction. The section during the forced state is assumed to keep a plane, and the average strain and average stress in each cell of the section obey the corresponding constitutive relationship of concrete or steel materials. The normal force and moment acting on the section are obtained by integrating on the section numerically to satisfy equilibrium and strain compatibility conditions as shown as below.

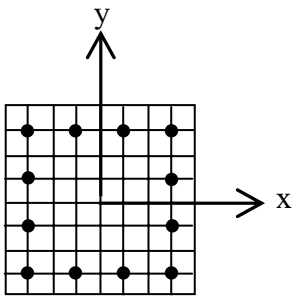

Figure 18 Dividing section on fiber elements in plastic hinge zone

$$\varepsilon = \bar{\varepsilon} + y\phi_x + x\phi_y \tag{30}$$

$$N = \int_A \sigma(\varepsilon(x,y))dA \tag{31}$$

$$M_x = \int_A \sigma(\varepsilon(x,y))ydA \tag{32}$$

$$M_y = \int_A \sigma(\varepsilon(x,y))xdA \tag{33}$$

$\bar{\varepsilon}$ = Average sectional strain

ϕ_x , ϕ_y = Section curvature in the x, y directions

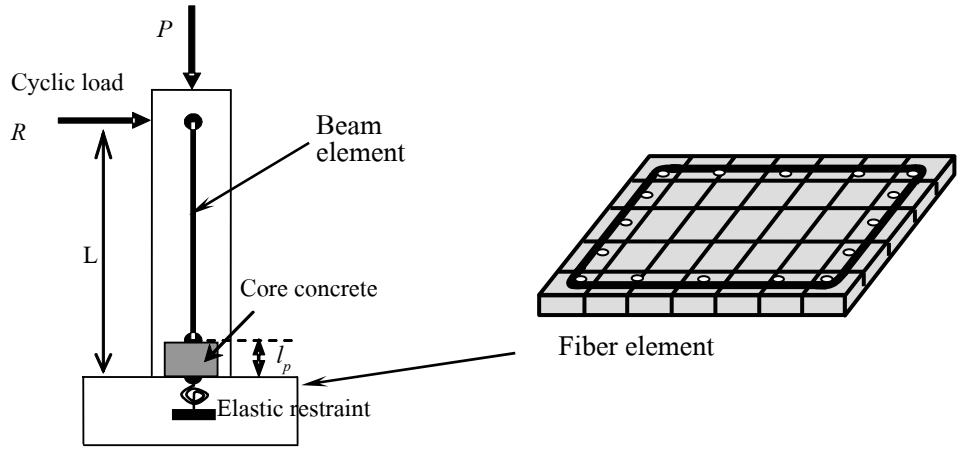

Figure 19 Analytical model

The structural model shown in Fig. 19 is a cantilever column consisting of a beam element and the confined plastic hinge zone at the base of column with length l_p. The plastic hinge zone is idealized by fiber elements having elastic rotation spring. The plastic hinge length of reinforced concrete members are calculated based on Paulay and Priestley (1992). This expression is given by

$$l_p = 0.08l + 0.022 d_b f_y \tag{34}$$

Nominal Shear Strength

The shear capacity for reinforced concrete members shall be conservatively based on the internal shear transfer of concrete and tie reinforcements. The nominal shear resistance of the members is provided (Priestley et al., 1994) as Equation (35)

$$V_n = V_c + V_s + V_p \tag{35}$$

In the Seismic Retrofitting Manual for Highway Bridges, Priestly method is adopted and the shear capacity components for rectangular are obtained as follows

$$V_c = v_c \times A_e$$
$$A_e = 0.8A_g$$
$$V_s = \frac{A_{sh} f_{yh} d}{s} \cot\theta$$
$$V_p = 0.2P$$

where

V_c = shear force carried by concrete

V_s = shear force carried by tie reinforcement

V_p = lateral component of compression strut in the column due to the applied compressive axial load

θ = the angle between the column axis and the diagonal concrete compression strut which is considered 45 degree in ACI-318

For plastic hinge region where the displacement ductility of the column $\mu_\Delta \geq 4$:

$$v_c = 0.1\sqrt{f_c'} \tag{36}$$

Based on Caltrans (2001), the concrete shear capacity of members designed for ductility shall consider the effects of flexure and axial load as specified in Equation (37).

For inside the plastic hinge zone is given by

$$v_c = Factor1 \times Factor2 \times \sqrt{f_c'} \leq 0.33\sqrt{f_c'} \tag{37}$$

and for outside the plastic hinge zone,

$$v_c = 0.25 \times Factor2 \times \sqrt{f_c'} \leq 0.33\sqrt{f_c'} \tag{38}$$

$$Factor1 = 0.025 \le \frac{\rho_s f_{yh}}{12.5} + 0.305 - 0.083\mu_d \le 0.25$$

$$Factor2 = 1 + \frac{P_c}{13.8 \times A_g} < 1.5$$

where

μ_d = local ductility demand defined by the ratio of the maximum displacement and the yield displacement

For members whose net axial load is in tension, $v_c = 0$.